CHAPTER 15

Three-Dimensional Reconstruction Methods for *Caenorhabditis elegans* Ultrastructure

Thomas Müller-Reichert[*], Joel Mancuso[†], Ben Lich[‡], *and* Kent McDonald[§]

[*]Medical Theoretical Center, TU Dresden, 01307 Dresden, Germany

[†]Gatan, Inc., Pleasanton, California 94588

[‡]FEI Company, 5651 Eindhoven, The Netherlands

[§]Electron Microscope Laboratory, University of California, Berkeley, California 94720

METHODS IN CELL BIOLOGY, VOL. 96

978-0-12-381007-6
DOI: 10.1016/S0091-679X(10)96015-9

Abstract

The roundworm *Caenorhabditis elegans* is one of the major model organisms in modern cell and developmental biology. Here, we present methods for the three-dimensional (3D) reconstruction of the worm ultrastructure. We describe the use of (1) serial-section analysis, (2) electron tomography, and (3) serial block face imaging by scanning electron microscopy (SEM). Sample preparation for high-pressure freezing/freeze substitution (HPF/FS) has been extensively covered in a previous volume of this "Methods in Cell Biology" series and will only be described briefly. We will discuss these 3D methods in light of recent research activities related to worm and early embryo biology.

I. Introduction

A. The Worm and Electron Microscopy—Some Early History

The history of *Caenorhabditis elegans* as a model system is also a history of using electron microscopy (EM) to understand three-dimensional (3D) cell relationships. From the beginning, EM was part of the plan for the worm as a model system (for historical perspective, see Brenner, 2009). The use of computers to aid in the reconstruction and analysis was planned as well, but the idea was mostly too far ahead of the hardware and software available at the time. Finally, the students, postdocs, and other associates working with Sydney Brenner used a combination of computer and manual methods to produce detailed reconstructions that were heroic in their scope and effort (Ward *et al.*, 1975; Ware *et al.*, 1975; White *et al.*, 1976). These culminated in the paper by White *et al.*, sometimes referred to as "The Mind of the Worm" (White *et al.*, 1986). This publication included 600 micrographs and 175 drawings of the *C. elegans* nervous system. Other publications followed, including David Hall's work on the EM reconstruction of the posterior nervous system that began as a thesis work at Cal Tech about this same period, and then published later (Hall and Russell, 1991).

However, with a few exceptions, EM was not to continue as a regular part of worm research. The pull of molecular genetics coupled with problems of development, physiology, neurobiology, and behavior took most worm researchers into areas where EM was not deemed essential. On the other hand, the worm is an excellent subject for light microscopy, and as light microscopes and reporter molecules evolved toward their current state, these tools were used to document nearly every aspect of worm structure and development that could be imagined. But while some thought (and some still think) that light microscopy would make EM obsolete, it has had precisely the opposite effect. Among all the many light microscope images of the worm that have accrued, there is a significant subset that comes up against the reality of resolution limits. True, there are some new developments in LM technology that are pushing beyond the old limits of 200 nm or so, but they will never get close to the resolution of the electron microscope. Fortunately, it is not an "either/or" type of situation, but one we could call "both/and." Today, we need to use both light and electron microscopy to fully understand the molecular basis for many biological events. More about this later, but we first need to understand why the specimen preparation for worm EM is so much better today than it was previously.

B. Worms Are Hard to Fix for EM but There Is a Solution

The role of EM may have continued to have been more integrated into the whole of worm research if it were not for the fact that the worm is extraordinarily difficult to fix well for ultrastructural studies. It is noteworthy that all the early studies were done with osmium as the primary fixative, even though glutaraldehyde was the general fixative of choice by that time. This may have actually been an advantage for cell lineage studies because the combination of extraction and high membrane contrast must have made it easier to follow cell connections. Later researchers found that by cutting open worms in the presence of glutaraldehyde, or glutaraldehyde plus osmium, they could get reasonable preservation of ultrastructure with less cytoplasm extraction (Hall and Russell, 1991). A summary of these fixation methods plus details of serial sectioning and 3D reconstruction methods was published by David Hall, and this work remains a valuable resource for anyone contemplating doing EM work on *C. elegans* (Hall, 1995). However, we now know that for the best possible preservation for EM studies, ultra-rapid freezing under pressures of about 2000 bar is the best choice. This technique is known as "high-pressure freezing" (HPF).

HPF was developed by Hans Moor at the Eidgenössische Technische Hochschule (ETH) in Zürich in the late 1960s (Moor and Riehle, 1968) and turned into a commercially available product in the mid/late 1980s (Moor, 1987). Fast-freezing methods for cytological preservation were well known in the 1960s and had their best applications in freeze-fracture studies that elucidated the basic structure of cell membranes. To prepare frozen samples for thin-section EM, it is usual to go through a process called "freeze substitution" (FS), whereby samples are dehydrated and fixed at low temperatures before warming up to higher temperatures for resin embedding and polymerization prior to sectioning. Martin Müller at the ETH pioneered in using HPF in combination with FS to visualize cell

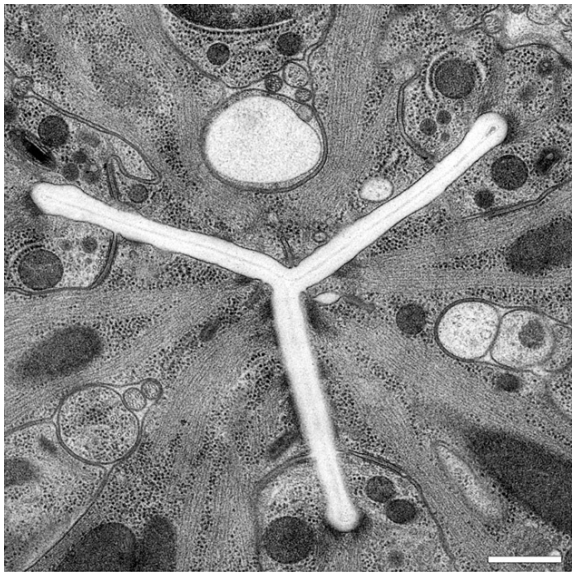

Fig. 1 Thin-section EM of a pharyngeal region of a wild-type dauer larva of *C. elegans*. The figure illustrates the quality of sample preparation after high-pressure freezing and freeze substitution in acetone containing 1% osmium tetroxide and 0.1% uranyl acetate. (Project with T. Kurzchalia, MPI-CBG, Dresden). Scale bar = 500 nm.

ultrastructure in thin resin sections (Müller and Moor, 1984; Humbel and Müller, 1986). Since the commercial availability of the BAL-TEC HPM 010 high-pressure freezer in 1985, there has been a slow but steady increase in the studies using HPF-FS to prepare samples for EM analysis (for a recent summary on HPF/FS, see: Humbel, 2009). The first studies to use HPF-FS for the study of worm ultrastructure and EM immunolabeling also came from the Müller laboratory (Favre *et al*., 1995, 1998; Hohenberg *et al*., 1994). For a review of how HPF has been applied to worm EM more recently, see the articles by Müller-Reichert (Muller-Reichert *et al*., 2003, 2008). The quality of ultrastructural preservation one can get with *C. elegans* samples is illustrated in Fig. 1.

At this point we must mention an alternative to HPF that can be used to preserve worm ultrastructure well. It is a technique developed recently by Leunissen and Yi (Leunissen and Yi, 2009) that they call "self-pressurized rapid freezing," or SPRF. In this method, worms are sealed in a small copper tube (16 mm long by 350 μm inner diameter) and plunged into liquid nitrogen, or cooled liquid propane. By a mechanism not well understood, a reasonable percentage of worms can be frozen without significant ice damage. SPRF might be a very inexpensive option for those worm laboratories wishing to carry out EM, but which do not have access to a high-pressure freezer. It should be mentioned that high-pressure freezers cost between US$ 140,000 and 240,000. On the other hand, the percentage of well-frozen worms possible by HPF is quite high and one can follow the same worm in LM and EM (Muller-Reichert *et al*., 2003).

C. Combining High-Pressure Freezing, Light Microscopy, and Electron Microscopy

Now that we know the best way to preserve worm ultrastructure, let us return to the subject of correlative light and electron microscopy (CLEM) as a powerful approach to answering basic questions about the molecular biology of the worm. There are different ways to define CLEM (McDonald, 2009), but for our purposes we mean that the same cells in the worm followed by LM are then observed in the EM. The next question is, how do we use HPF as the fixation tool in between the LM and EM observations? One answer is a relatively new type of HPF machine called the Leica EM PACT2+RTS. The RTS part of the name refers to the Rapid Transfer System, developed by Paul Verkade (University of Bristol, UK) to transfer a living sample from a light microscope to being high-pressure frozen within less than 5 s (Verkade, 2008). Applications to worm EM have been published previously (Muller-Reichert *et al*., 2007, 2008; Pelletier *et al*., 2006). CLEM of worms not requiring rapid transfer times can be done with any HPF machine as exemplified by the study of Sims and Hardin (2007). While CLEM has obviously the benefit of studying a tissue/or early embryo whose history is known and filmed, there is the added advantage that it greatly increases the sample size for EM studies. This is especially important if the subject of the study is of rare occurrence either spatially and/or temporally. With CLEM you can go to the electron microscope with confidence that you will be able to see the structure that you want to see.

D. A New Generation of 3D Reconstruction Tools for EM

Brenner originally included EM as part of his worm studies, but also mapping structures in three dimensions (see above). We have already discussed the fact that he was ahead of his time in using computers for making 3D reconstructions, but happily, computer hardware and software are now up to the task. Furthermore, we now have digital cameras of sufficient resolution that for most projects film is unnecessary. Without film we lose some resolution, but gain a lot of time between data collection and model building. What kinds of 3D imaging tools are available to the current generation of worm researchers interested in EM? We present four in this chapter: conventional serial-section reconstruction (Hall, 1995), electron tomography (ET; Frank, 1992), serial block face (SBF) imaging "a la Denk" (Denk and Horstmann, 2004), and focused ion beam (FIB) milling and imaging (Knott *et al*., 2008). The latter two methods use high-resolution scanning EM for imaging. Therefore, the resolution is less than transmission EM but for certain projects it is perfectly adequate and much faster. In summary, the two factors you need to consider when choosing a 3D reconstruction methods are (1) the resolution you need, and (2) the volume of structure you need to analyze.

E. 3D from Serial Thin Sections

As can be seen in Fig. 2, the *X*–*Y* resolution one can achieve with the different methods goes from the highest with ET and serial thin sectioning TEM, followed by FIB scanning electron microscopy (FIB-SEM) and SBF-SEM in the order of descending resolution. This figure includes a ranking for *Z*-resolution as well, but these

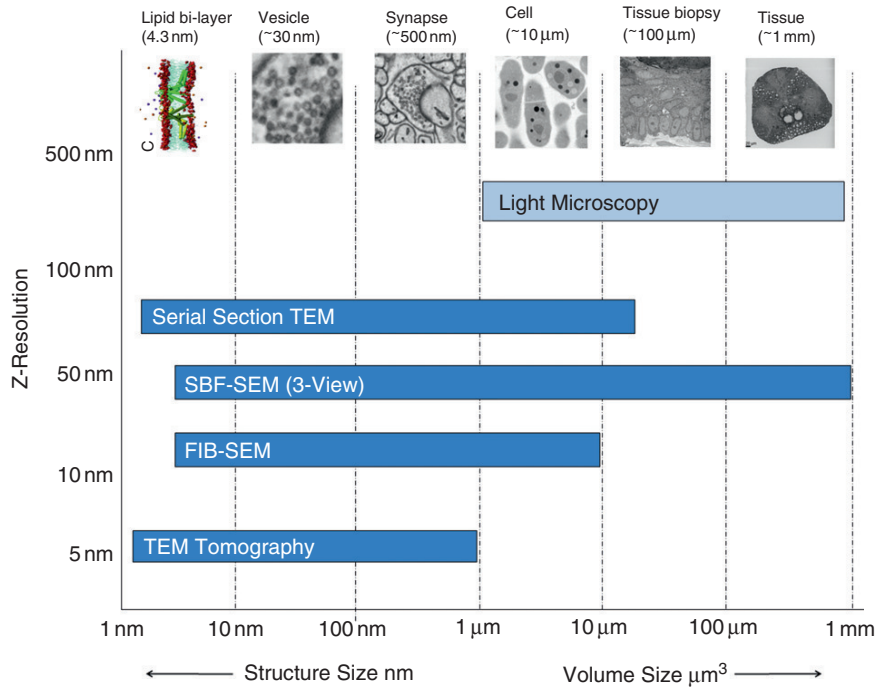

Fig. 2 Comparison of imaging methods for 3D analysis of biological samples. The methods basically differ in the volume that can be reconstructed and in the *Z*-resolution that can be obtained. (See Plate no. 15 in the Color Plate Section.)

numbers should be understood as approximations only. They will vary from sample to sample depending on factors, such as the section thickness chosen by the investigator, the density of the cytoplasm, or the quality of the microscope being used, among others. Within the SEM modes, the FIB-SEM can have the best *Z*-resolution because it can take such thin slices and the nature of the microscopes used, but the total volume reconstructed will be relatively small. The strength of SBF-SEM lies with the ability to reconstruct very large volumes.

Within the TEM modes, it is always best to use ET if possible, but there are situations where old-style serial-section reconstruction methods are preferable. The instance where this is most obvious is when one wants to reconstruct a structure that has a high axial ratio, i.e., the proportion of length to width. The worm is a perfect example of an organism with a high length-to-width ratio, and there are numerous examples of cellular components that can be tracked over distances of many hundreds of microns. The nervous system is historically the best example (see Brenner, 2009 and other citations given in the Introduction) but, as we will see, other cell types fit this criterion as well. While whole cells can be analyzed in 3D by serial ET (Hoog *et al.*, 2007; Marsh *et al.*, 2001), this approach is very labor intensive and typically can take months per single dataset. ET is in fact better suited for subcellular volumes that are at the level of organelles, such as the centrosome (O'Toole *et al.*, 2003; Pelletier *et al.*, 2006).

No discussion of serial-section analysis (SSA) of worms would be complete without mentioning the paper by Hall on this subject (Hall, 1995). Here the reader will find valuable tips on trimming, sectioning, picking up sections, poststaining, and how to recognize where you are when you are looking at the serial sections in the electron microscope. We will offer some alternative techniques for these subjects, but this paper must be read by anyone choosing to use serial thin sections for 3D reconstruction. Since 1995, a great deal has improved on specimen fixation as well as computer reconstruction methods, so these aspects of the Hall paper are a bit dated. The objective of this chapter is to bring these subjects up to date with the sections on HPF/FS and 3D reconstruction methods based on contemporary computer hardware and software. Fortunately, the software that has been developed for aligning and modeling tilt series in ET can be adapted for the same functions with serial thin sections.

It is worth mentioning at this point that serial sections are useful for things other than making 3D models. They can be used to quantify the numbers of organelles or other structures within a volume of the worm, or just to identify their presence or absence within. In addition, serial sections are useful for immuno-EM studies to check the specificity of the gold labeling.

F. Electron Tomography for 3D Modeling and Analysis

Electron tomography (ET) is a powerful method for 3D analysis, especially if one is interested in subcellular organelles at high resolution (Frank *et al*., 2002). Despite the ambitions of some researchers (Marsh *et al*., 2001; Noske *et al*., 2008; others), ET works best on volumes of a few square microns. There are some excellent recent papers on ET of the worm that illustrate this idea (O'Toole *et al*., 2003; Pelletier *et al*., 2006; Srayko *et al*., 2006; reviewed by Muller-Reichert *et al*., 2010). To perform ET at this level you will need an intermediate-voltage electron microscope, a good digital camera, and the appropriate computer hardware and software. Fortunately, most transmission EMs sold these days are outfitted for ET. Automated image acquisition programs are available from commercial vendors (FEI Company, Eindhoven, The Netherlands; Tietz Video and Image Processing Systems (TVIPS), Gauting, Germany). Several software packages are freely available (TOM, UCSF Tomography, and SerialEM, Boulder Laboratory for 3D Electron Microscopy of Cells). Depending on the organelle that you wish to reconstruct, there may or may not be software to help in the modeling phase of ET. This "segmentation" step remains a labor-intensive task for many projects.

G. Serial Block Face Reconstruction using Scanning EM (SBF-SEM)

To reconstruct local neural circuits, the SBF method was developed by Winfried Denk and Heinz Horstmann at the Max Planck Institute for Medical Research (Heidelberg, Germany) (Denk and Horstmann, 2004). A custom microtome is placed inside the specimen chamber of a scanning EM and a back-scatter detector is used to collect images of the block face (Fig. 3A). Then the block is sectioned in 30–200 nm

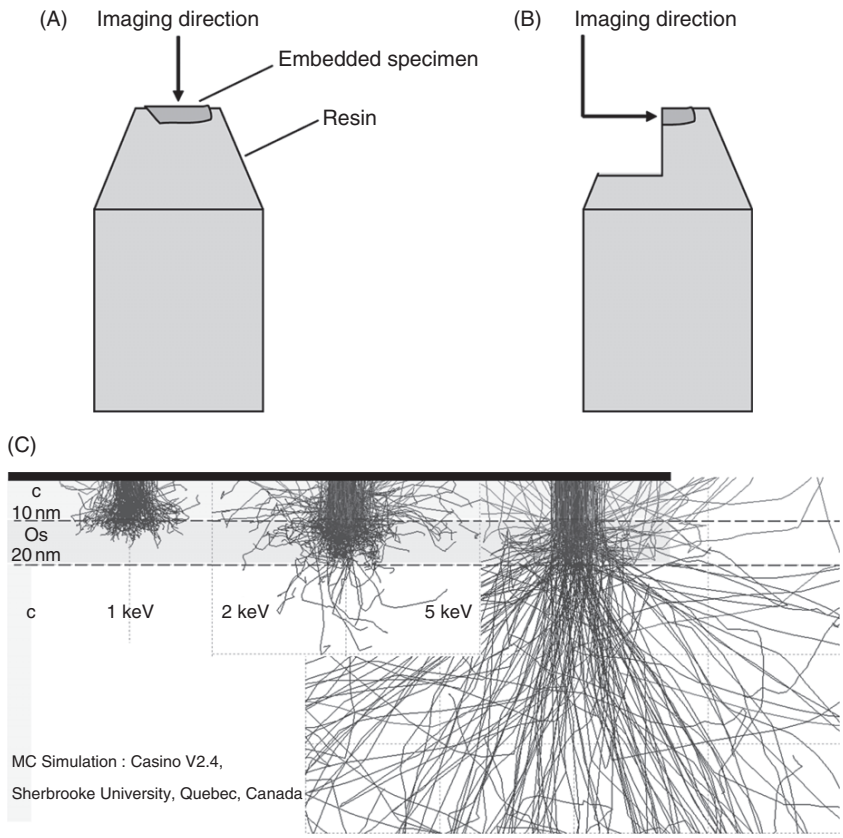

Fig. 3 Schematic diagram illustrating specimen orientation for block face imaging. (A) Serial block face SEM (SBF-SEM) using "3-View." The directions of sectioning and imaging are identical. (B) Focused ion beam SEM (FIB-SEM). The directions for FIB milling and imaging are perpendicular to each other. (C) Interaction of a 5-, 2-, and 1-keV primary electron beam with a carbon substrate as simulated using Casino v2.4.

increments, the section discarded, and the block face imaged again. There is currently a commercially available package for sectioning and data acquisition from Gatan, Inc., called "3-View," and we used this package for the work on SBF-SEM reported here.

Fixation strategies for SEM are the same as for TEM sample preparation. In principle, both HPF and traditional chemical fixation techniques are suitable for SBF-SEM. As mentioned above, HPF, however, is clearly the method of choice for the fixation of worm samples. Unlike conventional serial sectioning, SBF-SEM images the block face instead of the sections. Consequently, the SFB-SEM technique does not allow one to take advantage of postsectional staining, such as uranyl acetate or lead citrate. "*En bloc*" staining strategies have to be developed to maximize the back-scatter signal, thus improving resolution.

"3-View" can accommodate block faces up to 1×1 mm and can image large areas of the block at high resolution with a montage feature. For example, creating a 3×2 montage of $8k \times 8k$ images will give a field of view of 120×80 μm with a pixel size of 5 nm allowing the user to resolve mitochondrial cristae, microtubules, and synaptic vesicles.

Unlike other 3D imaging strategies, SBF-SEM raw images are perfectly aligned. Because the block face is imaged, and not the section itself, compression distortions, common in serial sectioning, are absent. In addition, because the block face itself is the focal plane of the microscope, no corrective focusing algorithms are necessary. Aligned sections can be viewed and scrolled through live during acquisition. "3-View" can acquire 1000–2000 $1k \times 1k$ serial images overnight using a standard beam current. Therefore, reconstructing large volumes from thousands of images becomes a streamlined and automated process when compared to manual techniques, such as serial-section TEM.

H. The Dual-Beam Focused Ion Beam Method (FIB-SEM) of 3D Modeling

Similar to the previous section, this is another method that uses SEM as the imaging tool, but rather than sectioning away material with an in-column microtome, an FIB is used to mill away material in between imaging steps. Compared to SBF-SEM imaging, the amount of material that can be removed per cycle is much less, and therefore the resolution in Z is improved accordingly. But like ET compared with serial-section reconstruction, the area that can be analyzed is relatively small. The achievable reconstruction volume for this technology is about one order of magnitude smaller than for serial sectioning, but about three orders of magnitude higher than for ET. The maximum surface using image tiling is approximately 100×50 μm with a pixel size as small as 2 nm. In the Z-direction, the number of slices is only time limited. The combination of ultra-thin serial sectioning with high-resolution back-scattered electron imaging enables acquiring datasets with isotropic voxels as small as 5 nm, allowing reconstructing a whole cell or multiple cells with adequate resolution for subcellular organelles.

The FIB in combination with a high-resolution scanning electron microscope (SEM) has proven to be very useful for obtaining high-resolution 3D data in an automated process (Knott *et al*., 2008). The principle of FIB-SEM is to remove serial slices of material and to image the block face as illustrated in Fig. 3B. The FIB is used for sectioning and allows cutting of ultra-thin sections that can be an order of magnitude thinner than sections cut by traditional ultramicrotomy. The FIB uses Ga^{2+} ions that are accelerated toward the sample. The gallium ion beam is scanned like in an SEM, and due to the mass and velocity of these ions, the material is removed by sputtering. By precisely scanning the FIB, the area of material removal can be controlled almost to the nanometer.

The SEM is used for imaging through back-scattered electrons. Importantly, in a biological specimen (prepared for TEM imaging) the contrast is created/increased by using heavy metals, such as osmium tetroxide, during the sample preparation process. The interaction of a 5-, 2-, and 1-keV primary electron beam with a carbon substrate is

simulated using Casino v2.4. These simulations show that a primary beam of lower energy yields a smaller interaction volume. Hence, the resolution that can be obtained from back-scatter imaging will improve with lower electron beam-accelerating voltages. Higher kV electron beam generates more signals from deeper layers in the specimen and hence "blurs" the structures close to the cross-sectional surface (Fig. 3C).

II. Rationale

Rationale of this chapter is to present and discuss methods for the 3D reconstruction of *C. elegans* ultrastructure. Specimen loading for HPF in combination with FS has been described in detail previously. Here, we give protocols for thin-layer embedding, CLEM, and the 3D reconstruction of cellular structures using SSA, ET, or SBF imaging by SEM.

III. Methods

A. High-Pressure Freezing and Freeze Substitution

As mentioned, these aspects of specimen preparation for HPF have been covered in detail in a number of recent publications (McDonald *et al*., 2007; Muller-Reichert *et al*., 2003, 2007, 2008). We will not repeat here what has been exhaustively covered previously. In brief, we routinely use 1% osmium tetroxide plus 0.1% uranyl acetate in anhydrous acetone for morphological studies (McDonald and Muller-Reichert, 2002). It is also possible to add up to 5% of water to the FS "cocktail" to increase membrane contrast (Buser and Walther, 2008).

In the following sections, we will, however, include those methods that are particularly useful for CLEM work and/or precisely oriented sectioning.

B. Thin-Layer Embedding

Labeled microscope slides are wiped clean with a soft cloth, submersed in a Teflon solution (MS-143V TFE Release Agent, Miller-Stephenson Chemical Co., Inc., Danbury, CT, USA), and allowed to dry. The slides are then polished to get a clean transparent surface, and two layers of Parafilm are placed on the margins of the glass slide to serve as spacers (Fig. 4A). About 200–300 µl of Epon/Araldite are placed on the microscope slide and allowed to disperse on the surface of the slide. Subsequently, specimen holders are placed in the resin droplet and held tightly with appropriate tweezers. Specimens are then removed from the sample holder (i.e., a membrane carrier for the EMPACT2 high-pressure freezer) with a sharpened tungsten needle or a comparable tool. Importantly, specimens tend to be brittle after FS, and care must be taken to avoid any mechanical damage to the embryo during these procedures. After removal of the empty membrane carrier, specimens in their final orientation are then softly pressed down to the surface of the glass slide, and

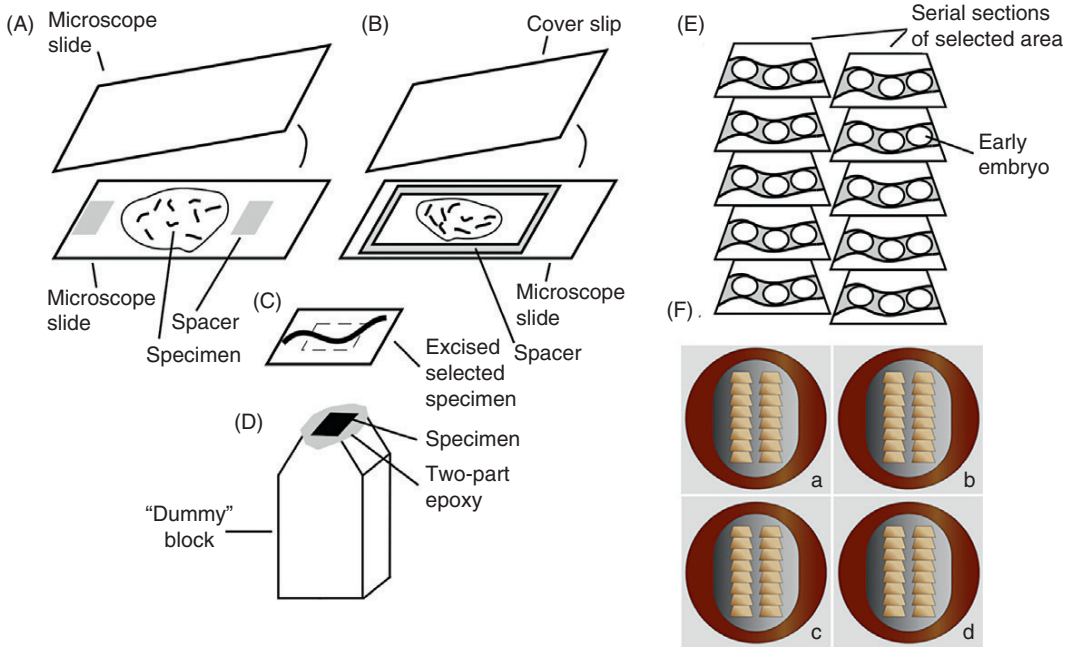

Fig. 4 Selection of thin-layer embedded *C. elegans* samples for electron microscopy. (A) Epon/Araldite-infiltrated samples are sandwiched between two Teflon®-coated microscope slides. Spacers are used to hold the slides apart. (B) For immuno-labeling, samples infiltrated with LR White resin are placed in slide molds made of a microscope slide and a Thermanox® spacer. Slide molds are closed using an Aclar® cover slip. (C) After polymerization of the resin, specimens are selected and excised. (D) Selected worms or early embryos are remounted on "dummy" blocks. (E) Serial sectioning of worms in longitudinal orientation. (F) Pairs of ribbons of serial sections can be placed on single EM grids. A whole series of serial sections (grids a–d) can be collected (Muller-Reichert *et al*., 2003). (See Plate no. 16 in the Color Plate Section.)

a second, coated and cleaned glass slide is put on top of the resin samples. This "sandwich" is placed on an appropriate support in the oven (about 48 h at 60°C) to polymerize the resin. One of the microscope slides is removed after resin polymerization by pressing a razor blade between the resin and one of the glass slides. At this stage, the microscope slide is suitable for screening in a light microscope and the specimens are ready for remounting on "dummy" blocks for ultramicrotomy (Muller-Reichert *et al*., 2003). A similar chamber can be made for samples infiltrated with LR White. Such samples are used for immuno-labeling experiments (Fig. 4B).

C. Screening and Remounting for Oriented Thin and Semi-Thin Sectioning

Polymerized samples are observed with a light microscope in bright field or with phase optics to relocate the specimens, whole worms, or capillary tubes with early embryos, for example, on the microscope slide (Muller-Reichert *et al*., 2003, 2007). An

objective marker with a diamond tip is used to mark a circle around the specimen. The purpose of this circling is threefold: (1) Whole worms or embryos in capillary tubes are clearly marked for handling in subsequent steps (i.e., during remounting). (2) The circle is used to determine the position of the specimen within the resin. By focusing up and down at high magnification, it can easily be determined on which surface of the thin resin layer the worm is located. Because most objects sink to the bottom of the resin layer prior to polymerization, they will always be at or near the surface and this must be known before remounting. By remounting the cells so they are at the upper surface, you can be cutting biological material in your first few sections. If you are cutting embryos inside the tubing, you can use the calibration of the *Z* movement on your microscope to estimate how far in the tubing you have to section before coming to the embryo. (3) The scribed circle can be used as an orientation aid. Marks can be scratched through the circle with a No. 11 scalpel blade to indicate particular orientations or subregions of the worm to be sectioned. Marks indicating where particular regions are located along the worm's long axis can help with rough trimming for serial cross sections (Muller-Reichert *et al*., 2007).

Using a scalpel, small squares of resin about 1×1 mm containing the specimen are cut out under a stereomicroscope. Miller-Stephenson (M-S) 907 Epoxy glue is used to remount the samples on "dummy" blocks. For serial longitudinal sections we mount the samples facing up (Fig. 4C–D); for serial cross sections we prefer to use dummy blocks from latex flat molds and glue the worm or early embryo on the side, rather than on top of the block. We prefer the M-S 907 glue because it can be sectioned and is stable in the electron beam. Polymerization of the glue at 60°C is completed within about 30 min. Remounted samples are then trimmed for thin sectioning.

D. Conventional Serial Thin Sectioning for 3D Reconstruction

1. Trimming Blocks for Conventional Serial Sectioning

a. Starting with the remounted sample(s) from HPF/FS-treated and thin-layer embedded material, the choice will be to trim for longitudinal or cross sections of the worm. Since Hall covered the cross-sectional approach so well, we will concentrate only on longitudinal sections of the worm (Hall, 1995). The instructions below are for sections of whole worms. Of course, if there are subsections along the length that are of particular interest, e.g., the spermatheca, or embryos at particular stages, then one can trim away the parts of the head and tail that are not of interest.

b. Rough trim with a single-edge razor blade, or even a jeweler's saw until there is an area of several hundred micrometers around each side of the worm.

c. For the final trimming switch to a very thin, double-edged razor blade such as the double-edged, stainless steel blades from Electron Microscopy Sciences, Cat. No. 72002 (Hatfield, PA, USA). These can be broken in half to form two single-edged blades by carefully folding the blade lengthwise while still in its wrapper until it snaps in two. Carefully remove the half blade from the wrapper and wipe the edge with ethanol-soaked laboratory tissue to remove grease from the manufacturer.

d. Under a stereomicroscope, either on the microtome or otherwise, trim away very thin (20 μm or so thick) slices parallel to the long axis of the worm until you are as close as you can get while still comfortable that you won't cut the worm itself. We would typically get within 50 μm or less. Pay careful attention to the reflectivity of the surface of this side of the block. It should be shiny and completely transparent so that you can see into the block. If it is opaque or rough in any way, then the blade is not sharp enough and you should move to an unused portion of the blade, especially for the final cut for this particular side.
e. Rotate the block 180° and repeat step 4 for the opposite side of the block. You should end up with parallel trimmed surfaces on either side of the worm. The final width will be determined by how much the body of the worm bends, if any.
f. Rotate 90° in either direction to trim the sides of what will be your final block face. We prefer to taper the sides so the final shape is an elongated trapezoid. Having these long top and bottom edges will help the subsequent serial sections stick to each other and form a ribbon.

2. Sectioning

g. Serial sections can be cut on almost any microtome, but we find that the Reichert-Jung (now Leica Microsystems, Vienna, Austria) Ultracut E to be particularly useful. This is because the sectioning arm and frame of the microtome are not connected, so this means you can rest your arm on the frame while the arm is cutting and it will not affect the sections. These microtomes come with a plastic shield that rests on the front platform, and we find this the best place to place our hand during sectioning. Other microtomes, including the newest models, tend to have mechanical connections between the frame and the arm so that any movement of the frame will affect the sections. Some have separate armrests that are connected only to the table, and if you do not have one of these models, consider making such an armrest.
h. Prepare Formvar-coated slot grids by whatever method you prefer. We like to make the films slightly thicker than we would use for mesh grids. The reflectance color on water should be solid silver, perhaps with a faint tinge of gold. Do not carbon-coat the filmed grids. This will only make them prone to becoming hydrophobic and very brittle. When carbon-coated slot grids are punctured, they will propagate a long split in the film and usually most sections are lost. With non-carbon-coated films, a puncture (say with a forceps tip) will just leave a hole and that hole can be "patched" by applying another, thinner layer of film over the hole and the sections can be saved. If grids are not to be used right away (within a day), store them in a refrigerator. This will keep them hydrophilic for several weeks in our experience. The exact duration varies with the humidity of the refrigerator, with more humidity working for longer times. We highly recommend using the Maxtaform copper–rhodium slot grids because each side is a different color. Put the film on the copper side.

i. Start sectioning the block at the preferred thickness. If the first few sections do not stick together, or if they are not coming off in a straight ribbon, then they must be adjusted accordingly. Retrimming the parallel sides should give straight ribbons. If the sections do not stick together, then there may be several reasons and remedies: (1) The parallel sides are not smooth enough due to a dull razor blade. Retrim with a new blade. (2) The water in the boat is not "conditioned." We have found that you sometimes have to break the surface tension in the boat by inserting a toothpick or another object into the boat. Watch the sections that are floating around when you do this, and if you see them rush forward toward the knife edge when you insert the toothpick, then you probably have corrected the problem. Often this has to be done twice or more before you see the sections move. Try not to introduce too much dirt with the stick. Cut a few more sections to see if they now come off as a ribbon. (3) If your microtome is equipped with an ionizer unit, try turning that on during sectioning. You can also place a polonium strip ionizer (GE Osmonics Labstore, Part. No. 1215174, 1-800-444-8212 in the U.S., and 1-952-988-6665 for international distributor information) near the knife and that may help.

j. By using an ocular with reticle, or by cutting a test ribbon, determine how many sections will fit within the 2-mm length of the oval slot. Also see if you can fit only one ribbon or more within the 1-mm width of the grid. All of this will vary, of course, depending on whether you are cutting longitudinal or cross sections and the size of the worm you are cutting.

k. When you reach the region of the worm where you are ready to start collecting sections, cut ribbons in lengths appropriate for the slot grid. As each ribbon comes to the proper length, use an eyelash or hair tool to dislodge it from the knife edge by gently touching the section just behind the one on the knife edge. Move the ribbon over to the side and continue cutting the next ribbon. If you rest your hand on the armrest you can do this without stopping and starting the microtome. As soon as you have enough sections/ribbons for one grid, move them over to the side of the boat. Continue like this until you have enough for four grids worth before stopping the microtome. The block should be stopped when it is below the knife edge but before it starts the return cycle. Using the fine control for retracting the arm, back it up 1–2 μm. Arrange the ribbons in pairs (Fig. 4E).

l. Next to the microtome you should have five pairs of forceps holding the slot grids. These should be numbered or marked so that you know the order they are in. Use forceps #1 to pick up the first set of sections cut. Insert the slot grid into the water at about a 45° angle and with the other hand use a hair tool to position the sections over the hole. Try to have the meniscus of the water at one edge of the slot and attach one edge of the ribbon raft to that part of the film. Then with a rolling and lifting motion, bring the grid out of the water so that the sections are over the slot. Carefully blot off excess water from underneath the grid with a laboratory tissue wrapped around a finger. Set this grid aside to dry and repeat with the remaining grids. Put them in a grid box in a known order after they dry (Fig. 4F).

m. Prepare five more slot grids in the forceps and have them next to the microtome. Resume sectioning and watch carefully as the block advances toward the knife. If

you see too much gap, advance the block manually, but as it gets close to cutting sections again just be patient and let it go until sections appear. With luck, you will continue to cut ribbons without a break from the previous series. If you do lose a section or two, make a note of it. Cut five more grids worth before repeating the last two steps.

3. Poststaining Grids

n. Stain sections using 1% uranyl acetate in 70% methanol for 10 min and Reynolds' lead citrate for 5 min. These times may vary depending on resin type and section thickness. We like to stain more than one grid at a time using a multiple grid staining device, such as the Pelco™22510 Grid Staining Matrix System (Ted Pella, Inc., Redding, CA, USA). We find most other devices for staining multiple grids to be inadequate because they tend to break the slots during loading and unloading.

4. Transmission Electron Microscopy

o. The first thing you must know when looking at serial sections on the microscope is the orientation, i.e., where are the first and the last sections. If you only have one ribbon and you have trimmed a trapezoid shape then there is no problem. With multiple ribbons you will have to determine which was cut first and last. You cannot rely on the arrangement that was in the boat, e.g., first ribbon on the right and second on the left with trapezoid pointing up, because different microscopes may or may not reverse that order as you see it on the screen or monitor. You will just have to check the continuity between the top section of one ribbon and the bottom section of its neighbor. When you get the correct order you may want to make a diagram that you can refer to in subsequent microscope sessions.

p. Grids without a carbon coat can be subject to charging and drift. However, there is something you can do that may stabilize the film. Go to the lowest magnification where you can still see the grid but not the objective aperture. Spread the beam to fill the field and use stage controls to irradiate all around the edge of the slot. Then, make several passes from one side of the slot to the other. If your magnification allows you to see the whole slot, then just leave the beam spread for several minutes as it irradiates the grid. This seems to stabilize the film and reduce problems with drift. If you have persistent drift problems, then you may have to carbon-coat the film, despite the other problems this might introduce.

q. It is a good idea to make a grid map, i.e., a diagram or a low-magnification image that shows the number of sections in each ribbon and the arrangement of ribbons. It is especially important if your ribbons are not perfectly aligned or if they have spaces between sections along their length.

r. Find areas of interest and start collecting serial images.

5. Three-Dimensional Reconstruction

s. We use the IMOD software package (Kremer *et al.*, 1996) to segment features of interest. The package allows the superposition of 2D traces to create a 3D representation of the subcellular structures. In addition, IMOD allows to correct some image distortions that arise during ultramicrotomy and imaging (Mastronarde *et al.*, 1993; McDonald *et al.*, 1992).

An example of 3D modeling from serial sections is given in Fig. 5 (Evans *et al.*, 2006). This figure shows a 3D reconstruction of amphid channel cilia in the worm "head".

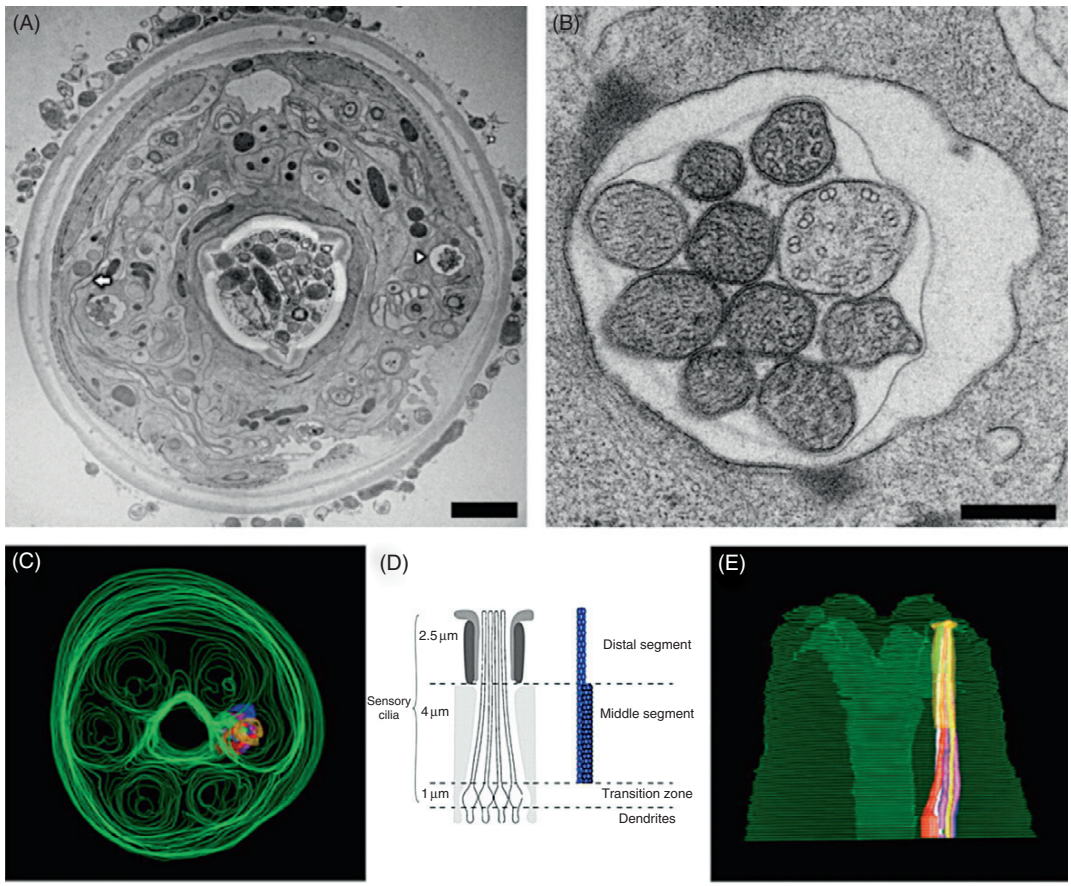

Fig. 5 Serial-section analysis of wild-type *C. elegans*. (A) Cross section through the head of a high-pressure-frozen/freeze substituted specimen embedded in Epon/Araldite. (B) Ultrastructure of the right amphid. (C and E) Top and side views of a 3D reconstruction from aligned serial sections showing overview of head and location of amphid channel cilia. Three-dimensional reconstruction was carried out using the IMOD software package. (D) Schematic illustration of channel cilia (from Evans *et al.*, 2006, with permission). (See Plate no. 17 in the Color Plate Section.)

E. Electron Tomography

All of the operations described above in sections III-D1–3, (Trimming blocks – post staining grids) can be used for preparing samples for ET with some slight variations. For HPF of early embryos, we use a correlative microscopy approach using a Leica EM PACT2+RTS high-pressure freezer. The method has been explained in detail previously (Muller-Reichert *et al*., 2007). For sectioning, we also use serial sections processed as described above, but we cut sections about 300 nm thick and usually put two ribbons in the center of a Formvar-coated copper 1×2 mm slot grid. The Formvar-film should have a "goldish" color. Using such prepared samples, we apply the following procedure:

1. Acquisition of Tomographic Data

a. Image a tilt series of semi-thick sections in an intermediate voltage (200–300 kV) EM equipped with a eucentric tilting stage. Collect serial, tilted views of the section every degree over a ±60° or 65° range.
b. After the first tilt series has been acquired, rotate the grid 90° to image a second tilt series over a ±60° or 65° range.
c. Use both tilt series to calculate a double-tilt tomogram as described (Mastronarde, 1997).

2. Segmentation and 3D Modeling of Microtubules

In the following paragraph, we briefly describe how to model microtubules in tomograms (O'Toole and Muller-Reichert, 2009). For the segmentation of other features, the reader is referred to published procedures (Ladinsky *et al*., 1999; Marsh *et al*., 2001).

d. Open the reconstructed volume using "3dmod" and go into model mode.
e. Create a model object and edit the object type as an open contour.
f. Open the slicer window and choose a microtubule by clicking the left mouse button. Rotate the *x, y*, and *z* sliders at the top of the slicer window to orient the microtubule along its long axis. Deposit model points along the microtubule using the middle mouse button. Each new microtubule modeled is a new contour in the object. In addition, create new objects for "open" and "closed" microtubule plus- and minus-ends. Deposit model points at each microtubule end. A projection of the 3D model can then be opened.
g. Different classes of microtubules (i.e., kinetochore microtubules, astral microtubules) are organized as separate objects and can be distinguished using different colors.
h. Once the microtubules in the volume have been modeled, a program can be run, mtrotlong, which will extract a series of subvolumes that contain the microtubules in a longitudinal orientation. The operator can then step through successive tomographic slices of the subvolumes to analyze the microtubule end morphology in detail.
i. Model objects can be displayed together or subsets of objects can be turned off or on to highlight the 3D relationships of particular features within the cell.

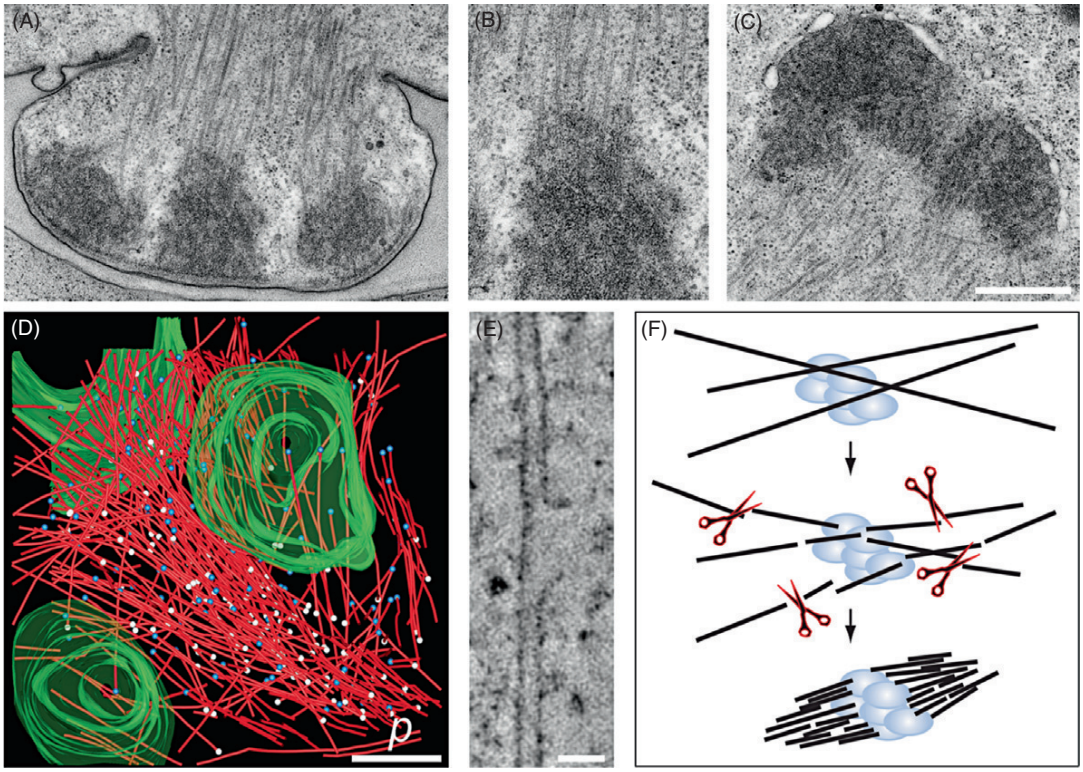

Fig. 6 Tomographic reconstruction of meiotic spindle assembly in *C. elegans*. (A–C) Thin-section EM showing a polar body, a kinetochore region with microtubules, and the formation of the female pronucleus. Scale bar = 500 nm. (D) Three-dimensional reconstruction of one half of a meiotic wild-type spindle (microtubules in red, pole-proximal ends as white spheres, pole-distal ends as blue spheres, chromatin in green, *p* is spindle pole) (Srayko *et al*., 2006). Scale bar = 500 nm. (E) Tomographic slice showing lateral disruption of the microtubule lattice (arrow). Scale bar = 50 nm. (F) Model explaining the role of *C. elegans* katanin in female meiotic spindle assembly (modified from Muller-Reichert *et al*., 2010). (See Plate no. 18 in the Color Plate Section.)

An example of the tomographic reconstruction of spindle microtubules in the early *C. elegans* embryo is given in Fig. 6. For details, the reader is referred to Srayko *et al*. (2006).

F. Serial Block Face SEM (SBF-SEM)

1. Specimen Preparation

Many of the procedures described above up until the point where the sample block is mounted for sectioning III-D1 (Trimming Blocks for Conventional Serial Sectioning) apply to sample preparation for SBF-SEM. What is different is that the contrasting in the material must be done prior to sectioning, and this may require some new "*en bloc*" methods. We applied contrasting during FS in 1% osmium tetroxide and 0.1% uranyl

acetate in anhydrous acetone (Muller-Reichert *et al*., 2003), but further protocols need to be developed (see discussion).

2. Specimen Trimming

Depending on the sample, the researcher may want to pre-screen the resin block by cutting thick sections for light microscopy to determine where in the biological material they want to start imaging in "3-View." Trimming should be such that the area of interest is surrounded by a large buffer zone, especially if the structure may move laterally as one proceeds in the *Z*-direction. For worms, it is simply a matter of leaving enough area of blank resin around the body of the worm that the worm itself will always be within the boundaries of the section.

3. Setting up the Instrument for Data Acquisition using "3-View"

Users will find setting up "3-View" to be familiar and almost identical to setting up a conventional ultramicrotome. Approaching the diamond knife to the 3-View sample resembles the same strategy as in a conventional ultramicrotome, using light reflections and shadows to align the diamond knife to a sample. Once the sample is within a few microns, the microtome is initialized to begin taking 200-nm cuts until the sample begins to cut. Once the microtome has begun to cut the surface, the chamber is pumped down and the user begins to search for an area of interest. 3-View software can be set up to automatically acquire an aligned 3D dataset. The user can choose the slice thickness, number of images, and the image size. Since the acquired images are aligned into stacks of images as they are acquired, the user can browse the 3D data life during the experiment.

SBF-SEM of worm samples is illustrated in Fig. 7 (see also Suppl. Movie 1 at http://www.elsevierdirect.com/companions/9780123810076). A dataset of 400 images was acquired with "3-View" in about 6 h. Figure 8 shows a manual segmentation of individual neurons from the dorsal nerve cord of *C. elegans*. For this particular dataset, segmentation was carried out using the Imaris software package (Bitplane, Zurich, Switzerland).

G. Focused Ion Beam SEM (FIB-SEM)

1. Sample Preparation for FIB-SEM

For the automated 3D data acquisition, the sample preparation can be kept almost identical to the sample preparation process for serial-section TEM analysis—up to the point where the sections are cut with the ultramicrotome (III-D1—Trimming Blocks for Conventional Serial Sectioning). The samples are processed for HPF/FS, thin-layer embedded, and mounted on "dummy" blocks. However, there is one modification to our standard embedding protocol: instead of embedding in Epon/Araldite, we follow the protocol by Knott for sample embedding in Durcupan (Knott *et al*., 2008). The FIB will cut the specimen perpendicular to the surface of the block (see above, Fig. 3B) and hence will create a cross-sectional surface for 3D imaging perpendicular to the plane that one would see with the TEM after taking ultra-thin microtome sections. Therefore, it is

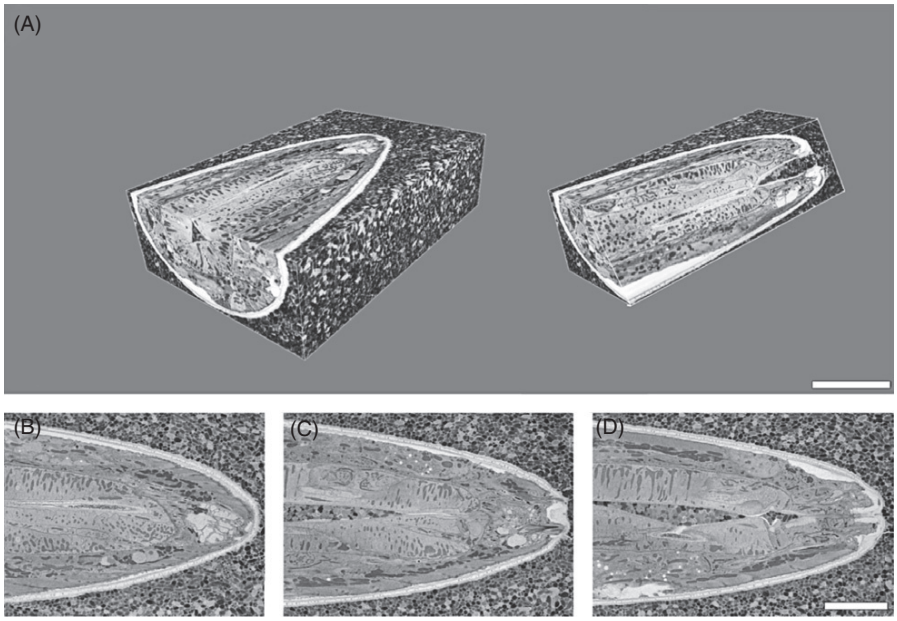

Fig. 7 Three-dimensional serial block face dataset of 400 images acquired with "3-View" of *C. elegans* in about 6 h. The slice thickness is 50 nm and the pixel size 50 nm as well, producing 50 nm isotropic voxels. 3D visualization and rendering was done using Imaris Bitplane software package. Scale bar = 250 μm. (B–D) Individual serial images of from the 3D data stack. Scale bars = 10 μm.

recommended to realize before mounting the specimen to the resin support what the ideal cut direction is and mount the specimen accordingly. The one step that differs for the sample preparation process for the Dual Beam is the removal of the mounting resin and some of the specimen, so that the volume of interest is as close as possible to the specimen surface (Fig. 9A–B). This is typically done using an ultramicrotome.

2. Setting up the Slice-and-View Process

The Dual Beam or FIB-SEM can be set up to automatically collect the 3D data by using the so-called "slice and view" process. This automated routine allows to set up (1) the slice thickness, (2) the amount of slices required, and (3) the field of view with the desired resolution. This automatic process allows overnight acquisition of data. A typical setup applied for studying the 3D architecture of subcellular organelles is using approximately 3 nm pixels in *X*–*Y* and a slice thickness of about 10 nm. This yields voxels of the size of $3 \times 3 \times 10$ nm. The "slice and view" process automatically prompts the user to go through all the required steps to get a successful dataset. It will create the FIB-removed trenches adjacent to the volume of interest for removed material to redeposit. Also it will prompt the system to deposit a layer of platinum on the top of the specimen for creating better cross sections with the FIB.

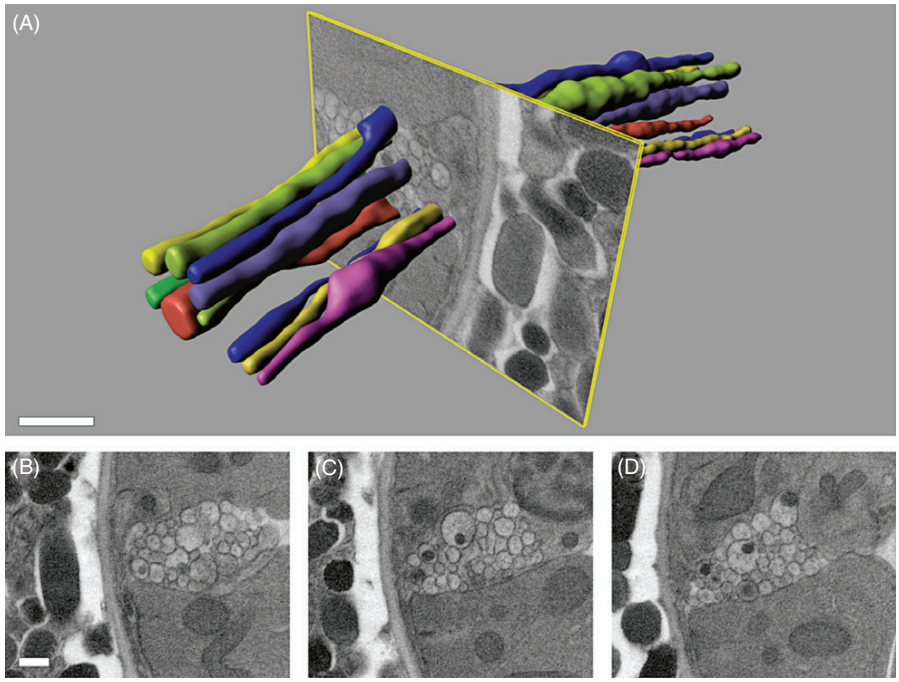

Fig. 8 Three-dimensional reconstruction by SBF-SEM using a Quanta 600 (FEI). (A) Small subset of 200 serial images visualized from a large 3D volume consisting of 1000 serial images. Individual neurons from the dorsal nerve cord of *C. elegans* have been manually segmentated using the Imaris Bitplane software package. Scale bar = 1 μm. (B–D) Individual serial images from the 3D data stack. Scale bar = 0.5 μm. (See Plate no. 19 in the Color Plate Section.)

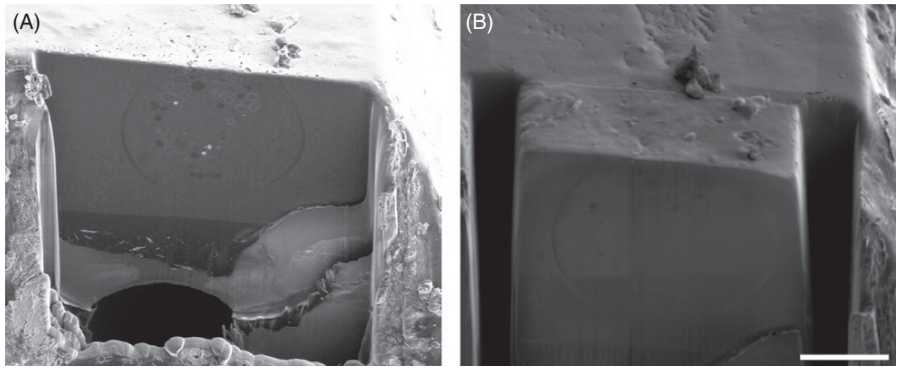

Fig. 9 Sample mounting for FIB-SEM. (A) The sample needs to be close to the resin surface. (B) Field of view at higher magnification. Scale bar = 10 μm.

An example of FIB-SEM is shown in Fig. 10. A larval worm (L3) was "sliced and viewed" in cross section. In this case, a layer of resin of 50 nm was removed per slice/view cycle, the voxel size was $13 \times 13 \times 50$ nm, and the sample was imaged at 2 kV.

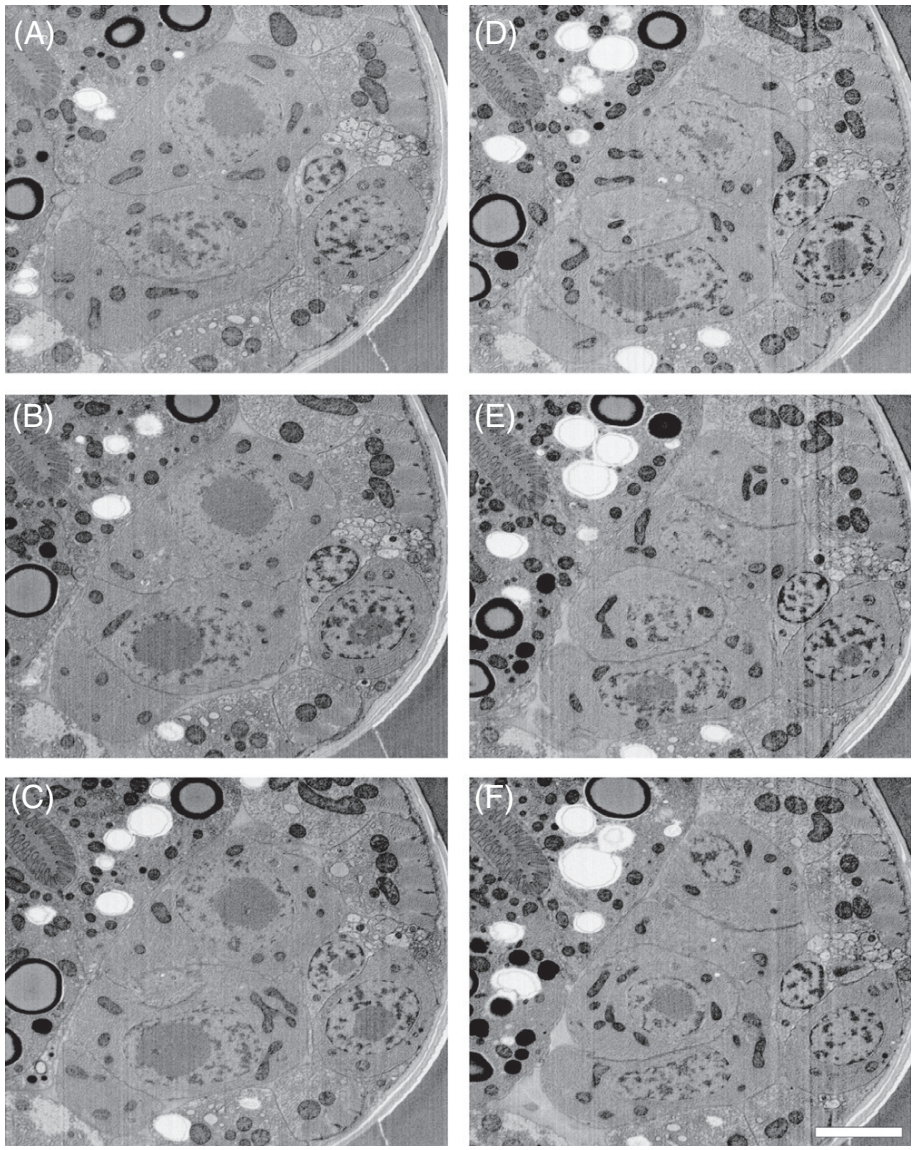

Fig. 10 Serial FIB-SEM slices through an L3 larva of *C. elegans*. This figure shows six images out of a series of 200 images. The sample was images with a Helios Nanolab 600 SEM operated at 2 kV. Slices of 50 nm were removed per cycle. Scale bar = 2.5 μm.

3. Three-Dimensional Reconstruction

As described above, the IMOD software package can be used to segment and model the features of interest (Kremer *et al*., 1996).

IV. Materials and Instrumentation

A. High-Pressure Freezing

Instrumentation: The currently available commercial high-pressure freezers include the ABRA HPM 010 (RMC-Boeckler, Tuscon, AZ, USA); the Wohlwend Compact HPF 01 (Wohlwend Engineering, Sennwald, Switzerland); the Leica EM PACT2 with or without the rapid transfer system (RTS) for specimen loading; and the Leica HPM 100 (Leica Microsystems).

Materials: For the EM PACT2 we use 100-μm-deep "membrane" carriers available from Leica Microsystems (McDonald *et al*., 2007). For the other instruments the least expensive source of specimen carriers is Wohlwend Engineering. One can get specimen carriers ranging in depths from 25 to 300 μm and we use the depth that most closely approximates the thickness of the worm generation that we are freezing. One can also use 3-mm EM grids as variable depth spacers as explained in detail elsewhere (McDonald *et al*., 2007, 2010). Tools for handling worms and specimen carriers include worm picks and an alcohol lamp, fine-tipped (sizes 0–00) paint brushes, micropipettors and tips, bibulous paper for wicking off excess liquid, and fine forceps for handling the specimen carriers during loading. An inexpensive, lower wattage dryer is best for warming and drying of specimen loaders.

Reagents: M-9 buffer (22 mM potassium phosphate monobasic [KH_2PO_4], 19 mM NH_4Cl, 48 mM sodium phosphate dibasic [Na_2HPO_4], 9 mM NaCl), bovine serum albumin (BSA) (Sigma-Aldrich, Steinheim, Germany). Air space in the carriers will cause poor freezing. To fill in the spaces between worms, we tend to use either thick *E. coli* paste from worm food plates (Muller-Reichert *et al*., 2003) or 20% BSA made up in M-9 buffer (Muller-Reichert *et al*., 2007).

B. Freeze Substitution

Instrumentation: Automatic FS device. Currently, one can get the AFS2 from Leica Microsystems or the EMS-002 Rapid Immersion Freezer with Freeze Substitution from Electron Microscopy Sciences. Alternatively, FS can be carried out on dry ice (for details, see McDonald, 1994).

Materials: Cryotubes.

Reagents: Anhydrous acetone (EM grade), osmium tetroxide, and uranyl acetate. The FS "cocktail" is made up ahead of time in cryotubes and frozen in LN_2, and the samples are added to the frozen fixative for either storage or just before starting FS. Details on making up fixatives can be found elsewhere (McDonald, 1999).

C. Thin-Layer Embedding

Instrumentation: Oven set at 60°C for polymerization.

Materials: Plastic beakers, transfer pipettes, a digital scale for weighing out components, magnetic stirrer, stir bars for mixing, waste containers, laboratory tissues, glass slides, polytetrafluoroethylene (PTFE) release agent (MS-143V, Miller-Stephenson Chemical Co., Inc.), lint-free cloth, air can, parafilm, and scissors.

Reagents: Epon 812 substitute, or Epon/Araldite mix, anhydrous acetone for making a graded infiltration series.

D. Screening, Remounting for Oriented Thin and Semi-Thin Sectioning

Instrumentation: Light microscopy equipped with phase optics to screen for samples, scribing tool that mounts on a light microscope objective turret (i.e., marker with a diamond tip, Leica), stereo microscope for remounting selected specimens, and ultramicrotome (preferably a recent model that will cut sections of consistent thickness). We use either an Ultracut E or an UCT ultramicrotome (Leica Microsystems).

Materials: Scalpel with No. 11 blade, remount glue (Epoxy 907 Adhesive System, Miller-Stephenson Chemical Co., Inc.), "dummy blocks", razor blades for trimming blocks, self-closing forceps (five pairs; Electron Microscopy Sciences, Cat. No. 72864-D), slot grids (Maxtaform copper–rhodium, 1×2 mm; Electron Microscopy Sciences, Cat. No. 2010-CR), and grid storage boxes.

Reagents: Formvar solution (0.5%; Electron Microscopy Sciences, Cat. No. 15820) and film casting accessories, uranyl acetate, lead citrate, and methanol.

E. Electron Tomography

Instrumentation: Intermediate-voltage electron microscope operated at 300 kV (we use a TECNAI F30 FEG, FEI Company, Eindhoven, The Netherlands), high-tilt rotating stage (Gatan model 650, Pleasanton, CA), 2K × 2K CCD camera (e.g., Gatan), image acquisition software package (SerialEM), and 3D reconstruction software (IMOD). Details can be found at http://bio3d.colorado.edu. In principle, ET can be done on most electron microscopes that are computer-controlled and fitted with digital cameras. As the acceleration voltage of the microscope goes up, the sample thickness can be thicker, and most ET is done these days with 200–400 kV instruments. The general "rule" is that the thickness of the sample (usually a resin section) in nanometers is roughly comparable to the kV of the microscope. Therefore, a 120-kV microscope could look at sections up to about 120 nm, a 300-kV scope could view 300 nm sections, and so on. The exact thickness of the sample will vary with the density of the sample, so low-density structures might be viewed in thicker sections.

Materials: Parafilm®, fine-tipped tweezers.

Reagents: 10- or 15-nm-colloidal gold (Ted Pella, Inc.).

F. Serial Block Face SEM (SBF-SEM)

Instrumentation: Scanning electron microscope. We used a Quanta 600 (FEI). "3-View" (Gatan) and Imaris software package (Bitplane, Saint Paul) was used.

G. Focused Ion Beam SEM (FIB-SEM)

Instrumentation: Scanning electron microscope. We used the Helios Nanolab 600 (FEI) for imaging.

V. Discussion

The choice of a 3D method is strongly dependent on the scientific question and, therefore, it is not really possible to give a general advice here on when to use which method for which biological project. We will instead give some method-related comments, which might help the reader to find the right method for her/his project.

1. Serial-Section Analysis

SSA is a rather "old" method. As mentioned earlier, it has been applied in the early days of *C. elegans* research to reconstruct the nervous system (Brenner, 2009), and the only complete wiring diagram of a neural circuit in existence is that of *C. elegans* (reviewed by Mishchenko, 2009). SSA is still very useful for reconstructing *C. elegans* ultrastructure (Evans *et al*., 2006), as well as that of other nematode species (Ragsdale *et al*., 2009). SSA is mainly applied when rather large structures have to be followed within the worm and modeled in 3D. In particular, SSA is useful when the length-to-width ratio for a structure is high. While it is possible to carry out serial ET through several sections (Hoog *et al*., 2007; Marsh *et al*., 2001; Noske *et al*., 2008), SSA is a more reasonable option when the number of sections required is tens to hundreds (see also Chapter 12 by Kang, 2010; this MCB volume). For the handling of large datasets, an interesting software package, called Collaborative Annotation Toolkit for Massive Amounts of Image Data (CATMAID), has been developed (Saalfeld *et al*., 2009).

SSA works particularly well when worms are mounted in a way that can be cut and imaged in cross section. We usually collect the ribbons for serial sectioning in pairs on filmed 1×2 mm slot grids. In general, the sectioning through whole worms is technically demanding and time consuming. In addition, there is always the danger of losing sections during ultramicrotomy and ribbon uptake, which results in "gaps" in the 3D reconstructions. To avoid loss of sections, automated high-throughput serial sectioning using the ATLUM approach (Automatic Tape-Collecting Lathe Ultramicrotome) has been developed. The ATLUM operation allows a spiral cut through a sample block, yielding a continuous ribbon of the biological material in the knife's water boat. The ribbons are collected by a submerged conveyor belt, allowing the production of ultra-thin section

libraries for imaging by SEM. For more information, the reader is referred to http://www.mcb.harvard.edu/lichtman/ATLUM/ATLUM_Web.htm. To our knowledge, this method has not been applied yet for either *C. elegans* worms or early embryos.

A different aspect that cannot be solved by continuous sectioning, however, is the fact that serial sections never fit perfectly when stacked *in silico*. The sectioning process itself induces some degree of compression, and the interaction of the electron beam with the plastic section causes both "global" and "local" distortions. Software packages, such as IMOD, allow to correct some of these distortions computationally (Mastronarde *et al*., 1993; McDonald *et al*., 1992). These distortions can be a serious problem when large areas have to be reconstructed in 3D.

2. Electron Tomography

The fact that the nematode worm develops in an amazingly stereotypical manner (Sulston and Horvitz, 1977) and the availability of a genome-wide RNAi screen, which allowed a classification of cellular defects from a collection of over 100,000 videos (Sonnichsen *et al*., 2005), made the early *C. elegans* embryo a popular model system for a number of cell biological questions. In recent years, we have used ET of plastic-embedded material for systematic structure and function analyses (reviewed by Muller-Reichert *et al*., 2010). In particular, we have analyzed the meiotic and mitotic spindle organization (O'Toole *et al*., 2003; Ozlu *et al*., 2005; Schlaitz *et al*., 2007; Srayko *et al*., 2006), the interaction of microtubules with kinetochores and centrosomes (O'Toole *et al*., 2003), and structural intermediates of centriole duplication (Pelletier *et al*., 2006). As mentioned, the volume that can be reconstructed by ET is rather small. In our studies, we have applied "montaging" of several tomograms in combination with serial tomography to enlarge the reconstructed volume, but we did not intend to reconstruct a whole mitotic spindle by ET (O'Toole *et al*., 2003). It is worth mentioning here that STEM tomography can be applied to use plastic sections with a thickness of up to 600 nm (Chapter 25 by Walther *et al*., 2010, this volume). To our knowledge, this method has not been applied so far for *C. elegans* samples.

It is important to note here that ET can also be applied to visualize frozen-hydrated samples in the TEM at liquid nitrogen temperature (Al-Amoudi *et al*., 2007; Beck *et al*., 2007; Medalia *et al*., 2002). Such samples for cryo-ET do not go through dehydration, fixation, or staining procedures as described for plastic embedding and have the potential to deliver images with higher resolution. Imaging of frozen-hydrated samples, however, has to be achieved at low-dose conditions (Al-Amoudi *et al*., 2004). Searching for specific "spots" within low-contrast cryo-sections of cells, however, is/remains a general problem of this method. Recently, it was hoped that tagging selected proteins by green fluorescent protein (GFP) might facilitate the identification of organelles in cryo-sections as visualized by deep-temperature light microscopy prior to ET (Gruska *et al*., 2008; Schwartz *et al*., 2007). It has to be kept in mind, however, that GFP signals in cells can be rather "weak" and that cryo-sections are usually much thinner compared to plastic

sections. In addition, serial cryo-sectioning is not a trivial task. When searching for a specific structure, such as the centrosome in the "huge" early embryo, is necessary, ET of plastic sections has certainly an advantage over cryo-ET.

We routinely use the IMOD software package, which contains all of the programs needed for calculating tomograms and for the display and modeling of subcellular features within the reconstructed volume (Kremer *et al*., 1996). The IMOD software package runs on multiple platforms, including Linux, Mac OSX, and Windows. The programs used for tomographic reconstruction are managed by a graphical user interface, eTomo. The eTomo interface facilitates the ease with which users go through the various steps of the process, much like a flow chart. Image display and modeling are carried out with the "3dmod" viewing program from the IMOD software package. This program can be run by command line; it contains windows for image display and the slicer tool for rotating slices of image data and for modeling features of interest in the reconstruction. Importantly, the IMOD software can also be used to model and reconstruct data obtained from either serial sectioning or block face imaging using SEM.

EM, using either of the methods presented above, delivers a high-resolution snapshot of biological samples, and this snapshot is ideally obtained by HPF of either whole worms (Muller-Reichert *et al*., 2003) or isolated, staged early embryos (Muller-Reichert *et al*., 2008). Biological processes, however, are dynamic and it is very powerful to combine the strength of the light microscope with the potential of the electron microscope. The general advantages of such a CLEM approach in combination with HPF have been highlighted recently (McDonald, 2009; Verkade, 2008). One of the most important, and often overlooked, aspects of CLEM is the ability to increase the sample size for EM analysis. Using CLEM methods means that you always know that your EM sample will contain exactly what you want to image. But if the feature of interest is small in size it may require pre-screening of serial semi-thick sections prior to carrying out ET (Muller-Reichert *et al*., 2007).

3. Block Face Imaging

As mentioned above, 3D reconstruction of whole worms can be achieved by SSA with the disadvantages that cutting of thin sections (i.e., 50–80 nm) is time consuming and demanding, and that images of serial sections do not allow a perfect superposition due to distortions. ET can be considered to take a somewhat "opposite position" to this. Very thin tomographic slices can be produced computationally (i.e., in the range of 2.5 nm). As mentioned, the volume of reconstruction is rather low, but can be increased by combining several datasets and applying "serial" ET (Hoog *et al*., 2007; Marsh *et al*., 2001; Noske *et al*., 2008). One would therefore hope to use a microscope where serial sectioning of rather thin slices is automated, and where the disadvantageous distortions due to the sectioning process can be avoided. Block face imaging by SEM is considered to occupy this "intermediate position." Using either SBF-SEM or FIB-SEM, the major advantage of this method is that imaging of the block face and not the section itself eliminates the creation of global and local distortions. The *Z*-resolution of

this technique basically depends on the thickness of the material that can be removed per cutting cycle, and it appears that the removal of the resin by a focused ion beam has an advantage over the use of an in-column microtome.

A problem that might occur with block face imaging is a rather low contrast of the biological specimen. In general, contrasting of samples as carried out for serial sections cannot be applied because the material is removed during each slicing step. We found that the contrast of samples after FS in acetone containing 1% osmium tetroxide and 0.1% uranyl acetate was acceptable for the imaging of cross sections of L3 larval worms. However, the contrast was not sufficient to visualize spindle microtubules in early embryos. Addition of 0.1% tannic acid to the FS "cocktail" obviously increases the contrast in mouse brain tissue prepared for block face imaging (Moebius *et al*., 2010, this volume). Further staining methods need to be developed in the future and will be critical for the success of block face imaging in general. We have also noticed that our routine Epon/Araldite recipe is not ideal for block face imaging by FIB-SEM. Instead, we followed the protocol published by Knott *et al*. to embed samples in Durcupan (Knott *et al*., 2008). Such prepared samples turned out to be harder and advantageous for the milling of material.

Segmentation of data obtained from SSA, ET, or block face imaging is currently the "bottleneck" in 3D reconstruction. When modeling spindle microtubules in tomograms, for example, the path of individual microtubules has to be modeled manually using the "slicer window" in IMOD (O'Toole and Muller-Reichert, 2009). It will be crucial for future studies to develop software packages that will allow the segmentation of organelles and even whole cells automatically (Sandberg, 2007). Efforts toward automation of segmentation are most likely the most important steps for future progress in the 3D EM field.

Acknowledgments

The authors would like to thank Jana Mäntler (MPI-CBG, Dresden) for excellent technical assistance. The lab of TMR is supported by the Deutsche Forschungsgemeinschaft (DFG MU 1423/2-1 and 1423/3-1).

References

Al-Amoudi, A., Diez, D. C., Betts, M. J., and Frangakis, A. S. (2007). The molecular architecture of cadherins in native epidermal desmosomes. *Nature* **450**, 832–837.

Al-Amoudi, A., Norlen, L. P., and Dubochet, J. (2004). Cryo-electron microscopy of vitreous sections of native biological cells and tissues. *J. Struct. Biol*. **148**, 131–135.

Beck, M., Lucic, V., Forster, F., Baumeister, W., and Medalia, O. (2007). Snapshots of nuclear pore complexes in action captured by cryo-electron tomography. *Nature* **449**, 611–615.

Brenner, S. (2009). In the beginning was the worm. *Genetics* **182**, 413–415.

Buser, C., and Walther, P. (2008). Freeze-substitution: The addition of water to polar solvents enhances the retention of structure and acts at temperatures around −60 degrees C. *J. Microsc*. **230**, 268–277.

Denk, W., and Horstmann, H. (2004). Serial block-face scanning electron microscopy to reconstruct three-dimensional tissue nanostructure. *PLoS Biol*. **2**, e329.

Evans, J.E., Snow, J. J., Gunnarson, A. L., Ou, G., Stahlberg, H., McDonald, K. L., and Scholey, J. M. (2006). Functional modulation of IFT kinesins extends the sensory repertoire of ciliated neurons in *Caenorhabditis elegans*. *J. Cell Biol*. **172**, 663–669.

Favre, R., Cermola, M., Nunes, C. P., Hermann, R., Muller, M., and Bazzicalupo, P. (1998). Immuno-cross-reactivity of CUT-1 and cuticlin epitopes between *Ascaris lumbricoides, Caenorhabditis elegans*, and *Heterorhabditis*. *J. Struct. Biol*. **123**, 1–7.

Favre, R., Hermann, R., Cermola, M., Hohenberg, H., Muller, M., and Bazzicalupo, P. (1995). Immuno-gold-labelling of CUT-1, CUT-2 and cuticlin epitopes in *Caenorhabditis elegans* and *Heterorhabditis sp*. Processed by high pressure freezing and freeze-substitution. *J. Submicrosc. Cytol. Pathol*. **27**, 341–347.

Frank, J. (1992). "Electron Tomography" Plenum Press, New York.

Frank, J., Wagenknecht, T., McEwen, B. F., Marko, M., Hsieh, C. E., and Mannella, C. A. (2002). Three-dimensional imaging of biological complexity. *J. Struct. Biol*. **138**, 85–91.

Gruska, M., Medalia, O., Baumeister, W., and Leis, A. (2008). Electron tomography of vitreous sections from cultured mammalian cells. *J. Struct. Biol*. **161**, 384–392.

Hall, D. H. (1995). Electron microscopy and three-dimensional image reconstruction. *Methods Cell Biol*. **48**, 395–436.

Hall, D. H., and Russell, R. L. (1991). The posterior nervous system of the nematode *Caenorhabditis elegans*: serial reconstruction of identified neurons and complete pattern of synaptic interactions. *J. Neurosci*. **11**, 1–22.

Hohenberg, H., Mannweiler, K., and Muller, M. (1994). High-pressure freezing of cell suspensions in cellulose capillary tubes. *J. Microsc*. **175**, 34–43.

Hoog, J. L., Schwartz, C., Noon, A. T., O'Toole, E. T., Mastronarde, D. N., McIntosh, J. R., and Antony, C. (2007). Organization of interphase microtubules in fission yeast analyzed by electron tomography. *Dev. Cell* **12**, 349–361.

Humbel, B. (2009). Freeze-substitution. *In* "Handbook of Cryo-preparation Methods for Electron Microscopy" (A. Cavalier, D. Spehner, and B. M. Humbel, eds.), pp. 320–341. CRC Press, Boca Raton.

Humbel, B., and Müller, M. (1986). Freeze substitution and low temperature embedding. *In* "The Science of Biological Specimen Preparation 1985" (J. J. Wolosewick, ed.), pp. 175–183. SEM, Inc., AMF O'Hare, Chicago, IL.

Kang, B.-H. (2010). Electron Microscopy and high-pressure freezing of *Arabidopsis*. *Methods Cell Biol*. **96**, 245–268.

Knott, G., Marchman, H., Wall, D., and Lich, B. (2008). Serial section scanning electron microscopy of adult brain tissue using focused ion beam milling. *J. Neurosci*. **28**, 2959–2964.

Kremer, J. R., Mastronarde, D. N., and McIntosh, J. R. (1996). Computer visualization of three-dimensional image data using IMOD. *J. Struct. Biol*. **116**, 71–76.

Ladinsky, M. S., Mastronarde, D. N., McIntosh, J. R., Howell, K. E., and Staehelin, L. A. (1999). Golgi structure in three dimensions: Functional insights from the normal rat kidney cell. *J. Cell Biol*. **144**, 1135–1149.

Leunissen, J. L., and Yi, H. (2009). Self-pressurized rapid freezing (SPRF): A novel cryofixation method for specimen preparation in electron microscopy. *J. Microsc*. **235**, 25–35.

Marsh, B. J., Mastronarde, D. N., Buttle, K. F., Howell, K. E., and McIntosh, J. R. (2001). Organellar relationships in the Golgi region of the pancreatic beta cell line, HIT-T15, visualized by high resolution electron tomography. *Proc. Natl. Acad. Sci. U. S.A*. **98**, 2399–2406.

Mastronarde, D. N. (1997). Dual-axis tomography: An approach with alignment methods that preserve resolution. *J. Struct. Biol*. **120**, 343–352.

Mastronarde, D. N., McDonald, K. L., Ding, R., and McIntosh, J. R. (1993). Interpolar spindle microtubules in PTK cells. *J. Cell Biol*. **123**, 1475–1489.

McDonald, K. L. (1994). Electron microscopy and EM immunocytochemistry. *Methods Cell Biol*. **44**, 411–444.

McDonald, K. (1999). High-pressure freezing for preservation of high resolution fine structure and antigenicity for immunolabeling. *Methods Mol. Biol*. **117**, 77–97.

McDonald, K. L. (2009). A review of high-pressure freezing preparation techniques for correlative light and electron microscopy of the same cells and tissues. *J. Microsc*. **235**, 273–281.

McDonald, K., Schwarz, H., Muller-Reichert, T., Webb, R., Buser, C., and Morphew, M. (2010). 'Tips and tricks' for high-pressure freezing of model systems. *Methods Cell Biol*. **96**, 639–660.

McDonald, K. L., Morphew, M., Verkade, P., and Muller-Reichert, T. (2007). Recent advances in high-pressure freezing: Equipment- and specimen-loading methods. *Methods Mol. Biol*. **369**, 143–173.

McDonald, K., and Muller-Reichert, T. (2002). Cryomethods for thin section electron microscopy. *Methods Enzymol*. **351**, 96–123.

McDonald, K. L., O'Toole, E. T., Mastronarde, D. N., and McIntosh, J. R. (1992). Kinetochore microtubules in PTK cells. *J. Cell Biol*. **118**, 369–383.

Medalia, O., Weber, I., Frangakis, A. S., Nicastro, D., Gerisch, G., and Baumeister, W. (2002). Macromolecular architecture in eukaryotic cells visualized by cryoelectron tomography. *Science* **298**, 1209–1213.

Mishchenko, Y. (2009). Automation of 3D reconstruction of neural tissue from large volume of conventional serial section transmission electron micrographs. *J. Neurosci. Methods* **176**, 276–289.

Möbius, W., Cooper, B., Kaufmann, W. A., Imig, C., Ruhwedel, T., Snaidero, N., Saab, A. S.., and Varoqueaux, F. (2010). Electron microscopy of the mouse central nervous system. *Methods Cell Biol*. **96**, 453–588.

Moor, H., and Riehle, U. (1968). Snap-freezing under high pressure: A new fixation technique for freeze etching. *In* "Electron Microscopy 1968. Pre-Congress Abstracts of Papers Presented at the Fourth European Regional Conference, September 1-7" (D. A. Bocciarelli, ed.), pp. 33–34. Tipografia Poliglotta Vaticana, Rome.

Moor, H. (1987). Theory and practice of high pressure freezing. *In* "Cryotechniques in Biological Electron Microscopy" (K. Zierold, ed.), pp. 175–191. Springer, Berlin, Heidelberg.

Müller, M., and Moor, H. (1984). Cryofixation of thick specimens by high-pressure freezing. *In* "The science of biological specimen preparation" (G.H. Haggins, ed.), pp. 131–138. SEM, Inc., AMF O'Hare, chicago, IL.

Muller-Reichert, T., Greenan, G., O'Toole, E., and Srayko, M. (2010). The *elegans* of spindle assembly. *Cell Mol. Life Sci*. **67**, 2195–2213.

Muller-Reichert, T., Hohenberg, H., O'Toole, E. T., and McDonald, K. (2003). Cryoimmobilization and three-dimensional visualization of *C. elegans* ultrastructure. *J. Microsc*. **212**, 71–80.

Muller-Reichert, T., Mantler, J., Srayko, M., and O'Toole, E. (2008). Electron microscopy of the early *Caenorhabditis elegans* embryo. *J. Microsc*. **230**, 297–307.

Muller-Reichert, T., Srayko, M., Hyman, A., O'Toole, E. T., and McDonald, K. (2007). Correlative light and electron microscopy of early *Caenorhabditis elegans* embryos in mitosis. *Methods Cell Biol*. **79**, 101–119.

Noske, A. B., Costin, A. J., Morgan, G. P., and Marsh, B. J. (2008). Expedited approaches to whole cell electron tomography and organelle mark-up *in situ* in high-pressure frozen pancreatic islets. *J. Struct. Biol*. **161**, 298–313.

O'Toole, E. T., McDonald, K. L., Mantler, J., McIntosh, J. R., Hyman, A. A., and Muller-Reichert, T. (2003). Morphologically distinct microtubule ends in the mitotic centrosome of *Caenorhabditis elegans*. *J. Cell Biol*. **163**, 451–456.

O'Toole, E., and Muller-Reichert, T. (2009). Electron tomography of microtubule end-morphologies in *C. elegans* embryos. *Methods Mol. Biol*. **545**, 135–144.

Ozlu, N., Srayko, M., Kinoshita, K., Habermann, B., O'Toole, E. T., Muller-Reichert, T., Schmalz, N., Desai, A., and Hyman, A. A. (2005). An essential function of the *C. elegans* ortholog of TPX2 is to localize activated aurora A kinase to mitotic spindles. *Dev. Cell* **9**, 237-248.

Pelletier, L., O'Toole, E., Schwager, A., Hyman, A. A., and Muller-Reichert, T. (2006). Centriole assembly in *Caenorhabditis elegans*. *Nature* **444**, 619–623.

Ragsdale, E. J., Ngo, P. T., Crum, J., Ellisman, M. H., and Baldwin, J. G. (2009). Comparative, three-dimensional anterior sensory reconstruction of *Aphelenchus avenae* (nematoda: Tylenchomorpha). *J. Comp. Neurol*. **517**, 616–632.

Saalfeld, S., Cardona, A., Hartenstein, V., and Tomancák, P. (2009). CATMAID: collaborative annotation toolkit for massive amounts of image data. *Bioinformatics*. **25**, 1984–1986.

Sandberg, K. (2007). Methods for image segmentation in cellular tomography. *Methods Cell Biol*. **79**, 770–799.

Schlaitz, A. L., Srayko, M., Dammermann, A., Quintin, S., Wielsch, N., MacLeod, I., de Robillard, Q., Zinke, A., Yates, J. R. III, Muller-Reichert, T., *et al.,* (2007). The *C. elegans* RSA complex localizes protein phosphatase 2a to centrosomes and regulates mitotic spindle assembly. *Cell* **128**, 115–127.

Schwartz, C. L., Sarbash, V. I., Ataullakhanov, F. I., McIntosh, J. R., and Nicastro, D. (2007). Cryo-fluorescence microscopy facilitates correlations between light and cryo-electron microscopy and reduces the rate of photobleaching. *J. Microsc*. **227**, 98–109.

Sims, P. A., and Hardin, J. D. (2007). Fluorescence-integrated transmission electron microscopy images: Integrating fluorescence microscopy with transmission electron microscopy. *Methods Mol. Biol*. **369**, 291–308.

Sonnichsen, B., Koski, L. B., Walsh, A., Marschall, P., Neumann, B., Brehm, M., Alleaume, A. M., Artelt, J., Bettencourt, P., Cassin, E., *et al.,* (2005). Full-genome RNAi profiling of early embryogenesis in *Caenorhabditis elegans*. *Nature* **434**, 462–469.

Srayko, M., O'Toole, E. T., Hyman, A. A., and Muller-Reichert, T. (2006). Katanin disrupts the microtubule lattice and increases polymer number in *C. elegans* meiosis. *Curr. Biol*. **16**, 1944–1949.

Sulston, J. E., and Horvitz, H. R. (1977). Post-embryonic cell lineages of the nematode, *Caenorhabditis elegans*. *Dev. Biol*. **56**, 110–156.

Verkade, P. (2008). Moving EM: The rapid transfer system as a new tool for correlative light and electron microscopy and high throughput for high-pressure freezing. *J. Microsc*. **230**, 317–328.

Walther, P., Wang, L., Liebem, S., and Frascaroli, G. (2010). Viral infection of cells in culture: Approaches for electron microscopy. *Methods Cell Biol*. **96**, 573–588.

Ward, S., Thomson, N., White, J. G., and Brenner, S. (1975). Electron microscopical reconstruction of the anterior sensory anatomy of the nematode *Caenorhabditis elegans*. *J. Comp. Neurol*. **160**, 313–337.

Ware, R. W., Clark, D., Crossland, K., and Russel, R. L. (1975). The nerve ring of the nematode *Caenorhabditis elegans*: Sensory input and motor output. *J. Comp. Neurol*. **162**, 71–110.

White, J. G., Southgate, E., Thomson, J. N., and Brenner, S. (1976). The structure of the ventral nerve cord of *Caenorhabditis elegans*. *Philos. Trans. R. Soc. Lond., B, Biol. Sci*. **275**, 327–348.

White, J. G., Southgate, E., Thomson, J. N., and Brenner, S. (1986). The structure of the nervous system of *Caenorhabditis elegans*. *Philos. Trans. R. Soc. Lond. [Biol.]* **314**, 1–340.